PROCEEDINGS OF SCIENCE

Measuring photon-induced tau-lepton pair production in ultra-peripheral heavy-ion collisions with ATLAS

Lydia Beresford, on behalf of the ATLAS Collaboration[a,*]

[a] *Deutsches Elektronen-Synchrotron DESY, Notkestraße 85, 22607 Hamburg, Germany*

E-mail: lydia.beresford@desy.de

Ultraperipheral lead-lead collisions at the LHC provide an intense flux of quasi-real photons. Collisions between these photons can yield the production of pairs of τ-leptons. This proceeding presents the first differential fiducial cross-section measurements of photon-induced di-tau production in lead-lead collisions at the LHC. The presented measurements utilise the full LHC Run 2 lead-lead dataset of 1.93 nb^{-1} recorded at $\sqrt{s_{NN}}$ = 5.02 TeV by the ATLAS detector.

The European Physical Society Conference on High Energy Physics (EPS-HEP2025)
7-11 July 2025
Marseille, France

[*] Speaker

PoS(EPS-HEP2025)197

1. Introduction

The Large Hadron Collider (LHC) is not only the highest energy proton-proton (pp) collider in the world, but also the world's highest energy lead-lead (Pb+Pb) collider. As the lead-ions are highly charged, they are surrounded by intense electromagnetic (EM) fields. These EM fields act as a cloud of quasi-real photons and high energy photon-photon collisions can occur. When the impact parameter between the lead-ions is greater than twice the ion radius, the collision is referred to as an Ultra-Peripheral Collision (UPC). UPCs are interesting as in this regime photon-photon collisions can dominate. Photon-photon collisions in Pb+Pb UPCs profit from a Z^4 cross-section enhancement, where Z is the atomic number and Z=82 for lead. Furthermore, they also profit from low trigger thresholds and negligible levels of hadronic pile-up compared to photon-photon collisions in pp data. The low thresholds enable access to unique low transverse momentum p_{T} phase space.

The ATLAS experiment [1] has been used to measure differential cross-sections for a range of UPC processes in $\sqrt{s_{NN}}$ = 5.02 TeV Pb+Pb collisions. This includes photon-induced di-electron $\gamma\gamma \rightarrow ee$ [2] and photon-induced di-muon $\gamma\gamma \rightarrow \mu\mu$ [3] processes. For the third generation τ-leptons, the photon-induced di-tau process $\gamma\gamma \rightarrow \tau\tau$, illustrated in Figure 1, was observed in Pb+Pb collisions by ATLAS [4] and CMS [6, 7], and in pp collisions by CMS [8]. Following observation, the results presented in this proceeding show the first differential $\gamma\gamma \rightarrow \tau\tau$ cross-section measurements in Pb+Pb collisions at the LHC [5].

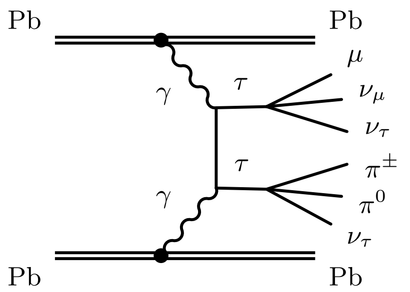

Figure 1: Example Feynman diagram for the photon-induced di-tau process $\gamma\gamma \rightarrow \tau\tau$ in Pb+Pb collisions. In this case, one tau-lepton τ decays to a muon μ, a muon neutrino ν_μ and a tau-neutrino ν_τ, the other tau-lepton τ decays to a charged pion $\pi^\pm$, a neutral pion π^0, and a tau-neutrino ν_τ. Figure from Ref. [5].

2. Experimental method

The measurement of differential $\gamma\gamma \rightarrow \tau\tau$ cross-sections in Pb+Pb collisions [5] utilises the full LHC Run 2 Pb+Pb dataset, comprising 1.93 nb^{-1} of Pb+Pb data recorded in 2015 and 2018 at $\sqrt{s_{NN}}$ = 5.02 TeV. The differential cross-sections are sensitive to the τ-lepton anomalous electromagnetic moments due to the two $\gamma\tau\tau$ vertices in Figure 1. They are also sensitive to spin correlation effects, τ-lepton decay modelling and the two-photon luminosity, which in turn depends on the photon-flux surrounding the ions and on the survival factor which governs the probability of ion break-up. The $\gamma\gamma \rightarrow \tau\tau$ signal process is estimated using Monte Carlo (MC) simulation, specifically, the nominal sample is generated using STARLIGHT 2.0 [9] with the photon-flux re-weighted to match that of the SUPERCHIC 3.05 generator [10]. TAUOLA [11, 12] is used to decay the τ-leptons and PYTHIA 8.245

[13] and PHOTOS++ 3.61 [14] were used to model final state radiation from the τ-leptons and the charged decay products of the τ-leptons, respectively.

The τ-lepton is the only lepton heavy enough to decay to hadronic final states. The τ-leptons in this analysis typically have low momentum, up to a few tens of GeV. Therefore, they are below the ATLAS hadronic tau reconstruction threshold. To identify $\gamma\gamma \rightarrow \tau\tau$ events electrons and muons with transverse momentum[1] $p_T(e/\mu) > 4$ GeV are utilised for leptonic decay modes and charged-particle tracks with $p_T(\text{trk}) > 100$ MeV are utilised to reconstruct hadronic decays as well as leptonic decay modes below the lepton reconstruction thresholds, referred to as low-momentum leptons throughout the rest of the proceeding. Three signal regions (SRs) are defined. The μe-SR selects events in which one τ-lepton decays to a muon plus neutrinos and the other τ-lepton decays to an electron plus neutrinos. The μ1T-SR selects events where one τ-lepton decays to a muon plus neutrinos and the other τ-lepton decays to a low-momentum lepton plus neutrinos or to a charged hadron plus a neutrino and potentially neutral hadrons. Finally the μ3T-SR selects events in which one τ-lepton decays to a muon plus neutrinos and the other τ-lepton decays to three charged hadrons, a neutrino and potentially neutral hadrons.

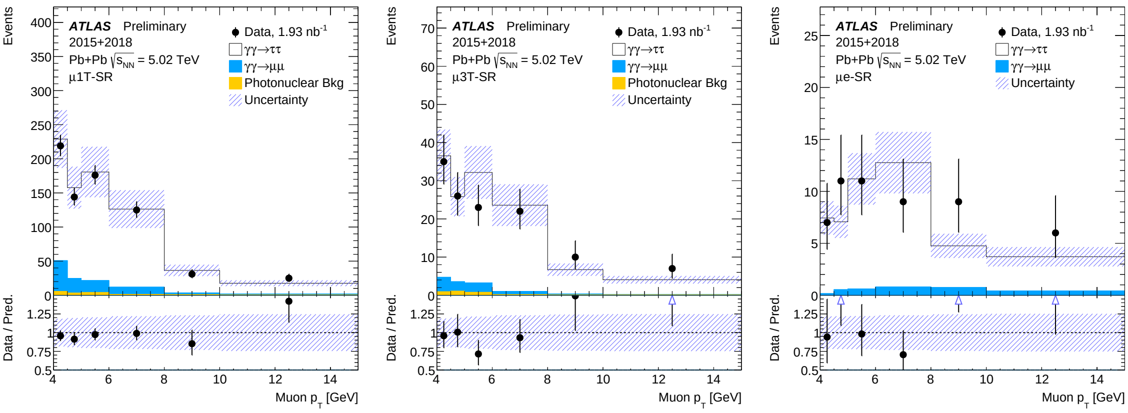

Figure 2: Detector-level muon p_T distribution in μ1T-SR (left), μ3T-SR (middle) and μe-SR (right). Figures from Ref. [5].

After applying event selection criteria, the main background process is photon-induced di-muon production $\gamma\gamma \rightarrow \mu\mu$. This process is estimated using MC simulation, specifically, the STARLIGHT generator is utilised and interfaced to PYTHIA 8 to model final state radiation from the muons. A dedicated $\gamma\gamma \rightarrow \mu\mu\gamma$ sample is produced using MADGRAPH5_AMC@NLO 2.9 [15]. Similarly to the signal sample, for the $\gamma\gamma \rightarrow \mu\mu(\gamma)$ samples the photon-flux is re-weighted to match that of the SUPERCHIC generator. The second largest background after event selection is the diffractive photo-nuclear background, which is estimated using a data-driven approach. The detector-level muon transverse momentum distribution in each SR are shown in Figure 2.

[1] ATLAS uses a right-handed coordinate system with its origin at the nominal interaction point (IP) in the centre of the detector and the z-axis along the beam pipe. The x-axis points from the IP to the centre of the LHC ring, and the y-axis points upwards. Polar coordinates (r, ϕ) are used in the transverse plane, ϕ being the azimuthal angle around the z-axis. The pseudorapidity is defined in terms of the polar angle θ as $\eta = -\ln \tan(\theta/2)$ and is equal to the rapidity $y = \frac{1}{2} \ln \left(\frac{E+p_z}{E-p_z} \right)$ in the relativistic limit. Angular distance is measured in units of $\Delta R \equiv \sqrt{(\Delta y)^2 + (\Delta\phi)^2}$.

Table 1: Truth-level object requirements and region selections for the fiducial regions are shown. Table adapted from Ref. [5].

Object	Requirements		
Leptons (e,μ)	$p_{\mathrm{T}} > 4$ GeV and $\lvert\eta\rvert < 2.5$		
Hadrons	$p_{\mathrm{T}} > 100$ MeV and $\lvert\eta\rvert < 2.5$		
Low-p_{T} Leptons (e_{low},μ_{low})	100 MeV $< p_{\mathrm{T}} <$ 4 GeV and $\lvert\eta\rvert < 2.5$		
Track particles (t)	Hadron or low-p_{T} lepton		
Region	μ1T-FR	μ3T-FR	μe-FR
0n0n topology	0n0n weights for MC		
N_μ	= 1	= 1	= 1
N_e	= 0	= 0	= 1
$N_t(\Delta R > 0.1$ from μ or $e)$	= 1	= 3	= 0
$\Sigma_{\mu,t(s)\text{ or }e}$ charge	= 0	= 0	= 0
$p_{\mathrm{T}}^{\mu,t}$	> 1 GeV	—	—
m_{3t}	—	< 1.7 GeV	—
$A_\phi^{\mu,t(s)}$	< 0.4	< 0.2	—

3. Differential cross-sections

Differential cross-sections are measured in three fiducial regions (FRs) referred to as μe-FR, μ1T-FR and μ3T-FR. The selections applied for these three regions, defined in Table 1, are similar to the object and signal region selections applied at detector-level. Transverse momentum p_{T} and pseudorapidity η requirements are applied to objects. For the fiducial regions, 0n0n weights derived from data and corrected for EM pileup are applied to re-weight the MC (which is generated inclusively in forward neutron topology) to a 0n0n topology with no forward neutrons detected by the Zero Degree Calorimeters on either side of ATLAS. Requirements are applied on the number of muons in the event N_μ, the number of electrons in the event N_e, the number of charged-particle tracks with $\Delta R > 0.1$ from the muon μ or electron e, and on the sum of charge over muons, tracks and electrons in the event $\sum_{\mu,t(s)\text{ or e}}$ charge. Furthermore, for μ1T-FR the muon-track system p_{T} must be above 1 GeV, for μ3T-FR the mass of the three track system must be below 1.7 GeV and for μ1T-FR and the μ3T-FR the acoplanarity between the muon and the track(s), which is defined as $A_\phi^{\mu,\mathrm{trk(s)}} = 1 - \lvert\Delta\phi(\mu,\mathrm{trk(s)})\rvert/\pi$, must be less than 0.4 and less than 0.2, respectively. In each FR, distributions for seven variables are measured to access kinematics of the $\gamma\gamma \to \tau\tau$ events. The distributions are unfolded using Bayesian iterative unfolding [16, 17] and the bootstrap method [18] to account for statistical correlations.

The differential cross-sections for the muon transverse momentum in each FR are shown in Figure 3. The unfolded data are compared to STARlight with the photon-flux re-weighted to match SuperChic plus Pythia 8, Tauola and Photos++ (blue triangles), STARlight with the photon-flux re-weighted to match SuperChic plus Pythia 8 and Photos++ (red triangles) and STARlight plus Pythia 8, Tauola and Photos++ (purple diamonds). The photon-flux depends on the nuclear charge distribution. For the STARlight generator the nuclear charge distribution is modelled as a point charge with a cutoff in impact parameter integration at the radius of the lead-ion. For SuperChic the charge distribution is modelled as a Woods-Saxon distribution with no cutoff in impact parameter integration. The unfolded data is seen to agree better with the simulated samples with the photon-flux re-weighted to match SuperChic. For the sample which uses the STARlight photon-flux, there is ~20% difference compared to the unfolded data due to the cutoff in impact parameter integration. This has also previously been observed in measurements of $\gamma\gamma \to ee$ and $\gamma\gamma \to \mu\mu$. The measurement is statistically limited with ~10-50% statistical uncertainty per bin and the total systematic uncertainty is ~5-10% per bin.

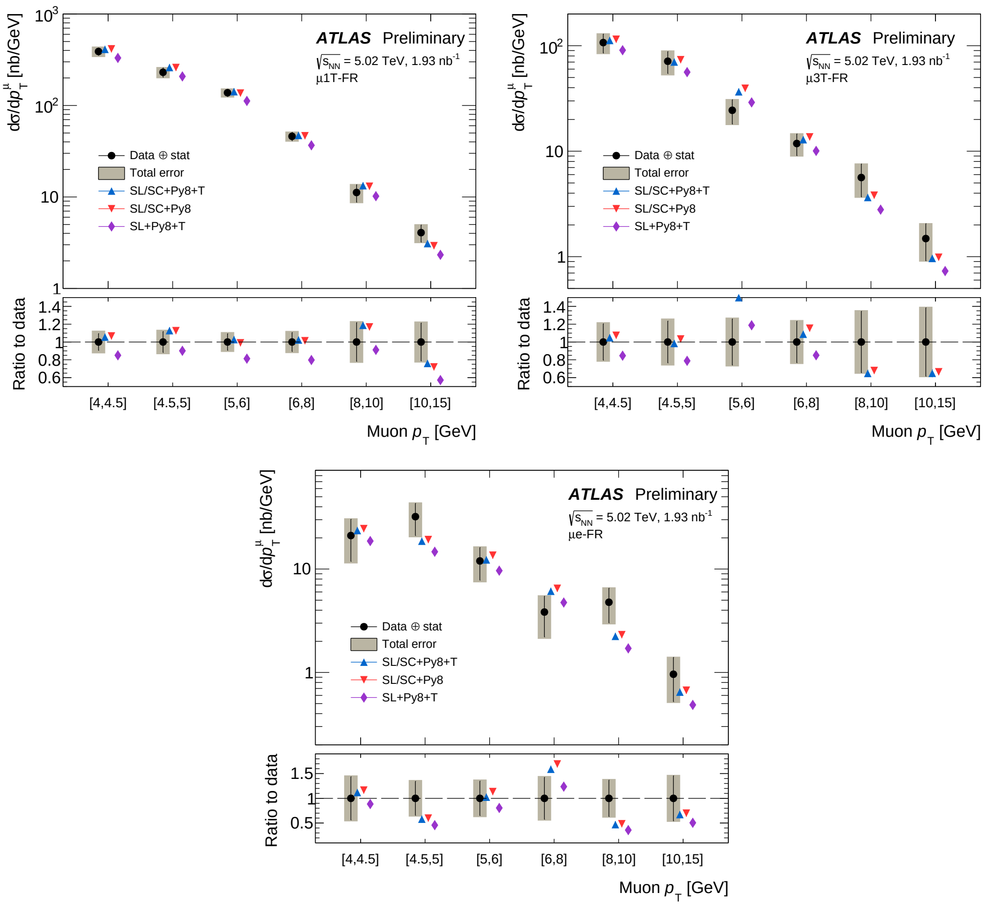

Figure 3: Differential cross-sections for muon p_T in μ1T-FR (top left), μ3T-FR (top right) and μe-FR (bottom). Figures from Ref. [5].

4. Conclusion

This proceeding presents the first differential cross-section measurements of $\gamma\gamma \to \tau\tau$ in UPC Pb+Pb collisions. The measurements are made using the full LHC Run 2 Pb+Pb dataset comprising 1.93 nb^{-1} recorded at $\sqrt{s_{NN}}$ = 5.02 TeV. In total 21 differential cross-sections have been measured, comprising seven variables in three Fiducial Regions. The differential cross-sections are sensitive to the τ-lepton electromagnetic moments as well as spin correlation effects, τ-lepton decay modelling and the two-photon luminosity.

References

[1] ATLAS Collaboration, *The ATLAS Experiment at the CERN Large Hadron Collider*, *JINST* **3**, S08003 (2008)

[2] ATLAS Collaboration, *Exclusive dielectron production in ultraperipheral Pb+Pb collisions at $\sqrt{s_{NN}}$ = 5.02 TeV with ATLAS*, *J. High Energ. Phys.* **06**, 182 (2023)

[3] ATLAS Collaboration, *Exclusive dimuon production in ultraperipheral Pb + Pb collisions at $\sqrt{s_{NN}}$ = 5.02 TeV with ATLAS*, *Phys. Rev.* C **104**, 024906 (2021)

[4] ATLAS Collaboration, *Observation of the $\gamma\gamma \to \tau\tau$ process in Pb+Pb collisions and constraints on the τ-lepton anomalous magnetic moment with the ATLAS detector*, *Phys. Rev. Lett.* **131**, 151802 (2023)

[5] ATLAS Collaboration, *Differential measurements of $\gamma\gamma \to \tau\tau$ using $\sqrt{s_{NN}}$ = 5.02 TeV Pb+Pb collisions with the ATLAS detector*, ATLAS-CONF-2025-004

[6] CMS Collaboration, *Observation of τ Lepton Pair Production in Ultraperipheral Pb-Pb Collisions at $\sqrt{s_{NN}}$ = 5.02 TeV*, *Phys. Rev. Lett.* **131**, 151803 (2023)

[7] CMS Collaboration, *Measurement of the tau g–2 factor in ultraperipheral PbPb collisions recorded by the CMS experiment*, CMS PAS HIN-24-011

[8] CMS Collaboration, *Observation of $\gamma\gamma \to \tau\tau$ in proton–proton collisions and limits on the anomalous electromagnetic moments of the τ lepton*, *Rep. Prog. Phys.* **87**, 107801 (2024)

[9] S. R. Klein et al, *STARlight: A Monte Carlo simulation program for ultra-peripheral collisions of relativistic ions*, *Comput. Phys. Commun* **212**, 258-268 (2017)

[10] L. A. Harland-Lang, V. A. Khoze and M. G. Ryskin, *Exclusive LHC physics with heavy ions: SuperChic 3*, *Eur. Phys. J.* C **79**, 39 (2019)

[11] S. Jadach et al, *The τ decay library TAUOLA, version 2.4*, *Comput. Phys. Commun* **76**, 361 (1993)

[12] N. Davidson et al, *Universal interface of TAUOLA: Technical and physics documentation*, *Comput. Phys. Commun* **183**, 821 (2012)

[13] T. Sjöstrand et al, *An introduction to PYTHIA 8.2*, *Comput. Phys. Commun* **191**, 159 (2015)

[14] N. Davidson, T. Przedzinski, and Z. Was, *PHOTOS interface in C++. Technical and physics documentation*, *Comput. Phys. Commun* **199**, 86 (2016),

[15] J. Alwall et al, *The automated computation of tree-level and next-to-leading order differential cross sections, and their matching to parton shower simulations*, *J. High Energ. Phys.* **07**, 079 (2014)

[16] G. D'Agostini, *A multidimensional unfolding method based on Bayes' theorem*, *Nucl. Instrum. Methods* A **362**, 487 (1995)

[17] G. D'Agostini, *Improved iterative Bayesian unfolding*, arXiv:1010.0632

[18] ATLAS Collaboration, *Evaluating statistical uncertainties and correlations using the bootstrap method*, ATL-PHYS-PUB-2021-011